Solving Poisson Equation with Slowing-down Equilibrium Distribution for Global Gyrokinetic Simulation

Qi Zhong, Yong Xiao[(*)]

Institute for Fusion Theory & Simulation

Zhejiang University, Hangzhou 310027

Abstract: A generalized multi-point average method has been developed for gyrokinetic Poisson equation with slowing-down equilibrium distribution and verified for its accuracy in the long and short wavelength limits, which forms an important basis for global gyrokinetic simulation of low frequency drift Alfvénic turbulence in burning plasmas.

Keyword: Gyrokinetics, Poisson Solver, Slowing-down Distribution

(*) Corresponding author: yxiao@zju.edu.cn

I. Introduction

In gyrokinetic particle simulation, the difference between particle distribution and gyro-center distribution leads to the double gyro-average of potential field, which is manifested in polarization density [1,2]. The polarization density, which is essential for gyrokinetic Poisson equation, depends critically on the phase structure of the equilibrium particle distribution, especially for short wavelength modes. Global gyrokinetic simulations are crucial for studying many important physics issues in magnetic fusion plasmas, such as turbulent transport scaling and turbulence spreading [3, 4, 5, 6, 7]. With the advent of burning plasmas, the alpha particles would inevitably excite Alfvenic turbulence with a slowing-down distribution via electron-alpha collisions [8, 9, 10, 11, 12, 13]. A more accurate global gyrokinetic Poisson solver with slowing-down background distribution is desirable for simulating alpha particle physics in burning plasmas and NBI heating scenarios.

Some recent researches have used so-called equivalent Maxwellian distribution, whose temperature or second order velocity moment is the same as slowing-down distribution [14] to simulate the alpha particle physics, which may be valid for a number for physics scenarios that depends weakly on the phase space structures of the equilibrium distribution. And

Some other work [15], though correctly consider velocity space derivatives in the gyrokinetic equations, uses flux-tube method to avoid tackling global spatial dependence of the gyrokinetic Poisson equation. In this paper, a novel global method based on multi-point average [2,16] to solve this equation is developed to adapt the slowing-down equilibrium distribution, and the accuracy of this new method is verified in the long and short wavelength limits. This method is essential for global gyrokinetic simulation to investigate alpha particle physics in the burning plasmas with the advent of ITER operation.

The rest of this article is structured as the following: Sec. II describes how to derive polarization density in gyrokinetics with slowing-down particle distribution; Sec. III shows our numerical scheme to solve gyrokinetic Poisson equation with the slowing-down equilibrium distribution; and numeric verification is provided in Sec. IV for the accuracy of this new scheme; The numerical results are summarized in Sec. V.

II. Gyrokinetic Poisson Equation

The gyrokinetic-Maxwellian system can be expressed as

$$\frac{\partial}{\partial t}\bar{f} + (v_\parallel \mathbf{b} + \mathbf{v}_d + \mathbf{v}_E)\cdot\nabla\bar{f} - \frac{\mathbf{B}^\star}{m_s B_0}\cdot\left(\mu_s\nabla B + q\left(\nabla\langle\delta\phi_{gc}\rangle + \mathbf{b}\partial_t\langle\delta A_{gc\parallel}\rangle\right)\right)\frac{\partial}{\partial v_\parallel}\bar{f} = 0, \quad (1)$$

$$q_i\delta n_i = e\delta n_e, \quad (2)$$

$$\nabla_\perp^2\langle\delta A_{gc\parallel}\rangle = \mu_0\sum_{s=i,e} q_s\delta u_{\parallel s} \quad (3)$$

where the gyro-center coordinates $(\boldsymbol{X}, v_\parallel, \mu, \zeta)$ are used, $\boldsymbol{v}_d = \boldsymbol{b}\times\left(\mu\nabla B + m_s v_\parallel^2\boldsymbol{\kappa}\right)/(q_s B)$ is magnetic drift for the guiding centers, $\mathbf{v}_E = -\nabla\langle\delta\phi_{gc}\rangle/B$ is the gyro-averaged $\boldsymbol{E}\times\boldsymbol{B}$ drift, and $\langle\dots\rangle$ represents gyrophase average. $\delta\phi_{\mathrm{gc}}$ is the perturbed potential at the gyro-center, which is defined as $\delta\phi_{\mathrm{gc}}(\boldsymbol{X};\mu,\zeta,t) \equiv \exp(\boldsymbol{\rho}\cdot\nabla)\,\delta\phi = \delta\phi(\boldsymbol{x},t)$ and the gyro-radius $\boldsymbol{\rho}$ is defined as $\boldsymbol{\rho} = \mathbf{b}\times\boldsymbol{v}_\perp/\Omega_s$, where the gyrofrequency $\Omega_{\mathrm{s}} = q_s B/m$ and magnetic moment $\mu_s = m_s v_\perp/2B$. And $\delta A_{gc\parallel}$ is perturbed parallel vector potential at the gyro-center. $\boldsymbol{B}^\star = \boldsymbol{B}_0 + m_\alpha v_\parallel\nabla\times\boldsymbol{b}/q_\alpha + \delta\boldsymbol{B}$. Suppose that the distribution function f can be decomposed into an equilibrium component f_0 and a perturbed component δf, i.e., $f = f_0 + \delta f$, the perturbed density δn_s can be calculated by $\delta n_s = \int d^3v\delta f_s$ and perturbed parallel fluid velocity $\delta u_{\parallel s}$ can be calculated by $\delta u_{\parallel s} = \int d^3v v_\parallel\delta f_s$. As is shown in Eq. (2), the quasineutrality for the fluctuating densities δn_s is used to solve for the electrostatic potential $\delta\phi$, which is valid for wavelengths longer than the Debye length. In many cases, the adiabatic response is assumed for electrons due to their fast parallel motion, i.e., $\delta n_{\mathrm{e}} = e n_0 \delta\phi / T_e$. In the last, the gyrokinetic parallel Ampère's law [17] in Eq. (3) is used for solving the vector potential $\delta A_{\|}$ and the gyrokinetic-Maxwellian system is closed.

Employing the Lie transform method [18], we can calculate the total ion density n_i by integrating over the velocity space a peculiar distribution function, which is generated by pulling back the gyro-center distribution function $\bar{f}$ into the particle coordinate space:

$$n_0 + \delta n_i = \int \mathrm{d}^3 v \exp(-\boldsymbol{\rho} \cdot \nabla) \left(1 + \frac{q_i}{B} \delta\tilde{\phi}_{\mathrm{gc}} \frac{\partial}{\partial\mu}\right) \bar{f}$$

Here $\delta\tilde{\phi}_{\mathrm{gc}} \equiv \delta\phi_{\mathrm{gc}} - \langle\delta\phi_{\mathrm{gc}}\rangle$ is the gyrophase dependent part of $\delta\phi_{\mathrm{gc}}$. It is found that the perturbed ion density δn_i can be separated into a perturbed guiding center density and a polarization density, i.e., $\delta n_i = \delta n_{i,\mathrm{gc}} + n_{i,\mathrm{pol}}$, where the guiding center density $\delta n_{i,\mathrm{gc}}$ is defined as $\delta n_{i,\mathrm{gc}} = \int \mathrm{d}^3 v \exp(-\boldsymbol{\rho} \cdot \nabla) \delta\bar{f}$, and the polarization density $n_{i,pol}$ is associated with the fluctuating electric field $\delta\phi$ through

$$n_{i,pol} = \int \mathrm{d}^3 v \exp(-\boldsymbol{\rho} \cdot \nabla) \left(\frac{q_i}{B} \delta\tilde{\phi}_{gc} \frac{\partial}{\partial\mu} f_0\right). \tag{4}$$

As for the parallel Ampère's law of Eq. (3), one can find that there's no explicit dependence on the perturbed electromagnetic field in the right-hand side of the equation, thus no extra modifications are needed when the equilibrium distribution function is changed from Maxwellian to slowing-down.

To solve the gyrokinetic Poisson equation, a proper numerical algorithm is needed to deal with the guiding center transformation $\exp(-\boldsymbol{\rho} \cdot \nabla)$ and gyrophase average in Eq. (4). The four-point gyro-average method has been invented [16] to solve the gyrokinetic Poisson equation in real space when the equilibrium distribution f_0 is Maxwellian, which enables a global gyrokinetic particle simulation [16,18]. Here we modify the original four-point average method to accommodate a slowing-down equilibrium distribution in order to investigate the self-consistent turbulent transport physics involving alpha particles, i.e., $f_0 = f_{sld}$.

The slowing-down distribution f_{sld} is the steady state solution to the collisional scattering for an isotopic particle source with a large birth speed v_0, i.e., the alpha particle speed produced by the thermal nuclear fusion, e.g., $\frac{1}{2}\mathrm{m}_\alpha v_0^2 = 3.5Mev$ for a typical D-T fusion. It is discovered that f_{sld} can be explicitly expressed as [19]:

$$f_{\mathrm{sld}}(v) = \frac{n}{4\pi I_1}\frac{H(v_0-v)}{v^3+v_c^3}, \tag{5}$$

where $v_c \equiv \left(\frac{3\sqrt{\pi}m_e}{4n_e}\sum_i \frac{q_i^2 n_i}{e^2 m_i}\right)^{1/3} v_{\mathrm{th},e}$ is the critical speed at which the electron drag is comparable to the thermal ion drag, and $I_1 = \frac{1}{3}\ln(1+v_0^3/v_c^3)$ is an auxiliary function for the purpose of normalization. A "temperature" can be defined for the slowing-down distribution as the 2nd velocity moment of the distribution function, which is similar to that of the Maxwellian:

$$\frac{3}{2}nT_{\mathrm{sld}} = \int \mathrm{d}^3v\frac{1}{2}m_i v^2 f_{\mathrm{sld}}(v) \equiv \frac{1}{2}nm_i v_c^2\frac{I_2}{I_1} \tag{6}$$

with $I_2 = \frac{v_0^2}{2v_c^2} - \frac{1}{6}\left(\frac{\pi}{\sqrt{3}} - 2\sqrt{3}\arctan\frac{1-2v_0/v_c}{\sqrt{3}} - \ln\frac{(1+v_0/v_c)^3}{1-v_0^3/v_c^3}\right)$. We note that for the fusion born alpha particles in a 10keV 50%-50% D-T plasma, $v_c/v_0 \approx 0.3$, $T_{\mathrm{sld}} \approx 1.28m_i v_c^2$.

Consider the Fourier representation of the perturbed potential $\delta\phi = \sum_k \delta\phi_k \exp(i\mathbf{k}\cdot\mathbf{x})$ in Eq. (4), and choose f_0 as the slowing-down distribution, then we can obtain:

$$n_{i,pol} = -\sum_k \int \mathrm{d}^3v\big(1-\exp(-i\mathbf{k}\cdot\boldsymbol{\rho})J_0(k_\perp\rho)\big)\delta\phi_k\lambda f_0\exp(i\mathbf{k}\cdot\mathbf{x})$$

$$= -\sum_k \big(c_0 - \Gamma_0(k_\perp\rho_c)\big)\frac{n_i}{T_i}q_i\delta\phi_k\exp(i\mathbf{k}\cdot\mathbf{x}), \tag{7}$$

where $\rho_c = v_c/\Omega_{\mathrm{I}}$, $\lambda = \frac{T_i}{m_i n_i}\left(\frac{3v}{v^3+v_c^3} + \frac{\delta(v_0-v)}{v}\right)$, $c_0 = \int \mathrm{d}^3v\lambda f_0 \equiv \frac{T_i}{m_i}\frac{I_3}{v_c^2 I_1}$ and $I_3 = \frac{1}{6}\left(\frac{\pi}{\sqrt{3}} - 2\sqrt{3}\arctan\frac{1-2v_0/v_c}{\sqrt{3}} + \ln\frac{(1+v_0/v_c)^3}{1-v_0^3/v_c^3}\right)$. $J_0 = J_0(k_\perp\rho_i) = \langle\exp(i\boldsymbol{k}\cdot\boldsymbol{\rho})\rangle$ is zeroth order Bessel function,, and $\Gamma_0(k_\perp\rho_c)$ is defined as

$$\Gamma_0(k_\perp\rho_c) \equiv \int \mathrm{d}^3v\exp(-i\mathbf{k}\cdot\boldsymbol{\rho})J_0(k_\perp\rho)\lambda f_0 = \int \mathrm{d}v_\perp v_\perp J_0^2(k_\perp v_\perp/\Omega_{\mathrm{i}})\tilde{f}(v_\perp), \tag{8}$$

which can be considered as the expectation of λ weighted by the equilibrium distribution f_0 after double gyroaveraging due to the back and forth transformation between particle position and gyrocenter position, where $\tilde{f}(v_\perp) = \int \mathrm{d}v_\parallel \lambda f_0$. In the case for f_0 to be Maxwellian, the function of Γ_0 can be calculated analytically [1], i.e., $\Gamma_0 = I_0(b)e^{-b}$, with $b = k_\perp^2\rho_t^2$ and $\rho_t = \sqrt{T/m}$. Unlike the Maxwellian equilibrium case, Γ_0 do not have a simple analytic expression in Fourier space when f_0 is slowing-down and has to be evaluated numerically. In principle, one can solve Eq. (2) using Eq. (7) and (8) in Fourier space. With these newly defined functions, the gyrokinetic Poisson equation can be written in a dimensionless form

$$\left(\frac{q_i}{T_i}c_0 + \frac{e}{T_e}\right)\delta\phi - \frac{q_i}{T_i}\widetilde{\delta\phi} = \frac{\delta n_{i,\mathrm{gc}}}{n_i}, \tag{9}$$

where $\widetilde{\delta\phi}$ has a complicated form in the real space but a neat form in the Fourier space:

$$\widetilde{\delta\phi} \equiv \sum_k \Gamma_0(k_\perp \rho_c)\delta\phi_k \exp(i\boldsymbol{k}\cdot\boldsymbol{x}). \tag{10}$$

However, this Fourier representation is not always valid since it mixes up the configuration space and velocity space dependences through J_0 term. In reality, the background magnetic field and perpendicular temperature can vary in real space, and then Γ_0 will gain global spatial dependences. Besides, the Fourier transform approach is more difficult to deal with realistic tokamak geometry, where no periodicity exists in the radial direction and on many occasions the global effects have to be considered seriously. For the Maxwellian background distribution, the four-point gyro-average method has been developed to solve this gyrokinetic Poisson equation in the real space [1,2]. Here we improve this method by including the slowing-down background distribution f_{sld} as the equilibrium distribution f_0 in the gyrokinetic Poisson equation, i.e., Eq. (9)

III. Gyrokinetic Poisson Solver with Slowing Down Distribution

The crucial part of implementing this gyrokinetic Poisson solver in the gyrokinetic simulation is to represent $\widetilde{\delta\phi}$ in Eq. (10) by the values of $\delta\phi$ at various field points in the real space. By numerical interpolation, we note that $\widetilde{\delta\phi}$ can be expressed as a linear combination of the $\delta\phi$ values on a number of nearby grid points and consequently Eq. (9) is transformed into a discrete matrix form such as $\mathbf{A}\cdot\mathbf{x}=\mathbf{b}$, which can then be solved by many known matrix inversion algorithms.

Starting from the definition of $\widetilde{\delta\phi}$ in its integral form instead of the Fourier form, one finds that

$$\widetilde{\delta\phi} = \int_0^\infty \mathrm{d}v_\perp v_\perp \langle \exp(-\boldsymbol{\rho}\cdot\nabla)\langle\delta\phi_{\mathrm{gc}}\rangle\rangle \tilde{f}(v_\perp). \tag{11}$$

To calculate $\widetilde{\delta\phi}$ at a grid point $\mathbf{x}_g$ for a specific $v_\perp$, one needs to evaluate the gyroaveraged function $\langle\exp(-\boldsymbol{\rho}\cdot\nabla)\langle\delta\phi_{\mathrm{gc}}\rangle\rangle$, which is the average value of $\langle\delta\phi_{\mathrm{gc}}\rangle$ on a ring with radius ρ

around $\mathbf{x}_g$, as is shown by the dotted circle in Fig. 1. The gyroaveraged quantity $\langle\delta\phi_{\mathrm{gc}}\rangle$ can also be calculated by this ring average method, e.g., the value of $\langle\delta\phi_{\mathrm{gc}}\rangle$ at the black triangle in Fig. 1 can be calculated by the average value of on solid circle. It is not necessary to actually integrate numerically along the whole ring to compute the gyrophase average, which would make the gyroaverage process rather time-consuming and expensive. According to [1, 2], A selection of four points uniformly distributed on the ring (four-point average method) is sufficient to compute the gyroaverage for wavelengths up to $k_\perp\mathrm{\rho}\sim 2$. Thus, nine neighboring points are required to compute $\widetilde{\delta\phi}$ on the grid point, as is shown by eight red points and the center blue diamond in Fig. 1. In more general geometry, these points required for the gyroaverage computation may not lay exactly on the grids, but their values can be acquired by a linear interpolation of the nearby grid points. Finally, summing up a few rings with different values $v_\perp$ with the weight function $\tilde{f}(v_\perp)$ and the relationship between $\widetilde{\delta\phi}$ and $\delta\phi$ on each grid point is found.

The remaining issue for evaluating Eq. (8) is how to discretize the $v_\perp$ integral with the weight function $\tilde{f}(v_\perp)$. Here we approximate the integral by a weighted summation by choosing a few sampling grid points along the $v_\perp$ coordinate. From the definition of $\widetilde{\delta\phi}$, one can tell that it is equivalent to approximate Eq. (8) by:

$$\Gamma_0(k_\perp\rho_c) = \int \mathrm{d}v_\perp J_0^2(k_\perp v_\perp/\Omega_{\mathrm{i}})\tilde{f}(v_\perp)$$
$$\approxeq \sum_j c_j J_0^2\left(k_\perp\mathrm{\rho}_c\frac{v_{\perp j}}{v_c}\right), \qquad (12).$$

where c_j are the summing weights due to $\tilde{f}(v_\perp)$ and $v_{\perp j}$ are the sampling grid points. The value pairs of $(c_j, v_{\perp j})$ are chosen by minimizing the following error function:

$$\epsilon = \int_0^a \left(\Gamma_0(x) - \sum_j c_j J_0^2\left(x\frac{v_{\perp j}}{v_c}\right)\right)^2 \mathrm{d}x \qquad (13)$$

Here a is the maximum value of $k_\perp\rho_c$ that we are interested in. Since low frequency micro-turbulence usually peaks around $k_\perp\rho_c < 1$, it is required that this approximation has a better accuracy for long wavelengths or $k_\perp\rho_c \ll 1$. Considering the Taylor expansion for $J_0(x)$ and $\Gamma_0(x)$ around $x\sim 0$, one finds that $J_0(x) = 1 - x^2/4 + O(x^4)$ and $\Gamma_0(x) = c_0 - \frac{T}{mv_c^2}x^2 + O(x^4)$. Let the first two terms equal to each other:

$$\sum_j c_j = c_0 = \frac{I_1 I_2}{3 I_1^2} \tag{14}$$

$$\sum_j c_j \frac{v_{\perp j}^2}{v_c^2} = \frac{2T}{m v_c^2} = \frac{2 I_2}{3 I_1} \tag{15}$$

These two constrains are then used to reduce degree of freedom. In order to minimize ϵ with respect to $(c_j, v_{\perp j})$, we use the Nelder-Mead method [19], which is a gradient-free iterative optimization algorithm. $I_{1,2,3}$ are functions of v_c/v_0, which is chosen to be 0.3 here to show numeric result of $(c_j, v_{\perp j})$. In the one-velocity-node case, we find that $c = 1.226$ with the velocity node $v_\perp/v_c = 1.443$ and the relative error is 3.6% for $k_\perp \rho_c < 0.5$. When using two velocity nodes, we find that $c_1 = 0.9347$ and $c_2 = 0.2910$ with the velocity nodes $v_{\perp 1}/v_c = 0.8778$ and $v_{\perp 2}/v_c = 2.510$, and the relative error is about 3.6% for $k_\perp \rho_c < 1.5$. In the three-velocity-node case, we find that $(c_1, c_2, c_3) = (0.1186, 0.3881, 0.7190)$ with $(v_{\perp 1}/v_c, v_{\perp 2}/v_c, v_{\perp 3}/v_c) = (0.7016, 1.716, 2.984)$, and the relative error is only 0.46% for $k_\perp \rho_c < 2$. The three-velocity-node approximation is compared with the exact value from direct numerical integration, as is shown in Fig. 2. Satisfactory accuracy is achieved with a relative error less than 0.46% for $k_\perp \rho_c < 2,$ which is sufficient to include most interesting finite Larmor radius effects due to the slowing-down alpha particles. We also test for the widely used Padé approximation for the thermal ions, and finds that it can introduce a 10% relative error near $k_\perp \rho_c \sim 1.5$ comparing to the exact solution. Fig. 3 shows the comparison between the four-point average method and the Padé approximation with the following form

$$\Gamma_0(k_\perp \rho_c) = \frac{c_0}{1 + \frac{1}{c_0} \rho_c^2 k_\perp^2}. \tag{16}$$

We note that the Padé approximation with the Maxwellian distribution has a similar form with $c_0 = 1$. In the long wave length limit, these approximations are both very close to the exact value, as is shown in Fig. 3, and it can be further verified by the numeric benchmarks shown in the next section.

IV.Numeric Verification

To verify our global algorithm for the slowing down background distribution, we shall solve the gyrokinetic Poisson equation without electron response in a large-aspect-ratio toroidal geometry with circular cross section as a sample problem. In the long wavelength limit, Eq. (9) can be reduced to the following form using Taylor expansion of Γ_0:

$$\frac{q_i}{m\Omega_\mathrm{i}^2}\nabla_\perp^2\delta\phi=-\frac{\delta n_{i,\mathrm{gc}}}{n_i} \tag{17}$$

Toroidal effect can be ignored and $\nabla_\perp^2=\frac{1}{r}\frac{\partial}{\partial r}r\frac{\partial}{\partial r}+\frac{1}{r^2}\frac{\partial^2}{\partial\theta^2}$ in polar coordinates on poloidal cross section. After these simplifications, Eq. (17) is just a normal Poisson equation and we can choose $\delta n_{i,\mathrm{gc}}$ to be the eigenfunction of the Laplacian operator to ensure an analytic solution. Let $\delta n_{i,gc}/n_i=\big(J_m(k_0r)-Y_m(k_0r)J_m(k_0a_1)/Y_m(k_0a_1)\big)\cos m\theta$ in which k_0 satisfies $J_m(k_0a_0)Y_m(k_0a_1)-Y_m(k_0a_0)J_m(k_0a_1)=0$. Then the solution of this Poisson equation is just $\delta\phi=k_0^{-2}\big(J_m(k_0r)-Y_m(k_0r)J_m(k_0a_1)/Y_m(k_0a_1)\big)\cos m\theta$ with zero boundary condition on $r=a_0,a_1$. With $m=6$ as an example, the comparison between analytic solution and numeric solution along the line $\theta=0$ is shown on Fig. 3., where a perfect match is found between them. More generally, the poloidal cross section contour for the solution is shown on Fig. 4. The difference between the analytic 2D solution and numerical one is negligibly small, as is shown by Fig. 4(c). Thus, in the long wavelength limit, our four-point average method works perfectly for the slowing down equilibrium distribution.

In order to simulate short wavelength modes, we need to verify the validity of our algorithm in the short wavelength limit. The verification process is getting subtle in the short wave length limit, since there's no analytic solution for $\delta\phi$ when expanding the Γ_0 operator in this limit. But we can still compare the numerical solutions to Eq. (12) by the developed four-point average with the Padé approximation. We solve Eq. (9) with a natural unit $T_i=T_e=q_i=e=1$, and a short-wave-length density fluctuation $\frac{\delta n}{n_i}$, which is in the same form as that in long-wave-length limit but with much larger m and k, i.e., $\mathrm{k_r}\rho_c=1\sim2, m=62\sim125$. As is shown in Fig. 5 and 6 for three cases with different $k_r\rho_c$, The solutions from these two different numeric schemes show little difference, suggesting that they can both handle the short wave length case within an acceptable error of 5%. The amplitude of the solution using four-point average method is slightly larger, which can be ascribed to the fact that this operator of four-point average is larger than the Padé approximation in the k space, as is shown in Fig. 2.

V. Conclusion

A real space gyrokinetic Poisson solver for slowing-down equilibrium distribution has been developed based on the multi-point average method [2,16] and verified for its accuracy in the long and short wavelength limits. The discovery process for this method is shown in detail and it can be further modified to accommodate more equilibrium particle distributions. This method can be incorporated in the global gyrokinetic particle simulation to study the crucial alpha particle physics in the burning plasmas, i.e., to simulate the drift Alfvenic turbulence accurately in the presence of slowing-down alpha particle distribution.

Acknowledgement

This work is supported by National MCF Energy R&D Programme of China Nos. 2019YFE03060000 and 2015GB110000, and by NSFC under Grant No. 11975201.

Reference

1. W. W. Lee, Phys. Fluids 26, 556 (1983).
2. W. W. Lee, J. Comput. Phys. 72, 243(1987)
3. Z. Lin, T. S. Hahm, S. Ethier, and W. M. Tang, Phys. Rev. Lett. 88, 195004 (2002).
4. W. X. Wang, Z. Lin, W. M. Tang, W. W. Lee, S. Ethier, J. L. V. Lewandowski, G. Rewoldt, T. S. Hahm, and J. Manickam, Phys. Plasmas 13, 92505 (2006)

5. J. Lang, Y. Chen and S. Parker, Phys. Plasma 14, 082315 (2007)
6. L. Qi, J. M. Kwon, T. S. Hahm, S. Yi, and M. J. Choi, Nucl. Fusion 59, 026013 (2019).
7. T. S. Hahm, P. H. Diamond, Z. Lin, K. Itoh, and S.-I. Itoh, Plasma Phys. Control. Fusion 46, A323 (2004).
8. X Wang, F. Zonca, L. Chen, Plasma Phys. Control. Fusion 52, 115005 (2010)
9. A. Bierwage, L. Chen, and F. Zonca, Plasma Phys. Control. Fusion 52, 015005 (2010)
10. L. Chen and F. Zonca, Rev. Mod. Phys. 88, 015008 (2016)
11. W. W. Heidbrink, Phys. Plasma 15, 055501 (2008)
12. W. Shen, F. Wang, G. Y. Fu, L. Xu, G. Li and C. Liu, Nucl. Fusion 57, 116035 (2017)
13. He Sheng and R.E. Waltz, Nucl. Fusion 56, 056004 (2016)
14. Estrada-Mila, Candy, and Waltz Phys. Plasma 13, 112303 (2006)
15. C. Angioni and A. G. Peeters, Phys. Plasma 15, 052307 (2008)
16. Z. Lin and W. W. Lee, Phys. Rev. E 52, 5646 (1995)
17. I. Holod, W. L. Zhang, Y. Xiao, and Z. Lin, Phys. Plasmas 16, 122307 (2009)
18. R. G. Littlejohn, J. Math. Phys. 23, 742 (1982)
19. P. Helander, D. J. Sigmar, Collisional Transport in Magnetized Plasmas. United Kingdom: Cambridge University Press (2005)
20. Nelder, J. A. and Mead, R. Comput. J. 7, 308-313, 1965.

VI. Figures

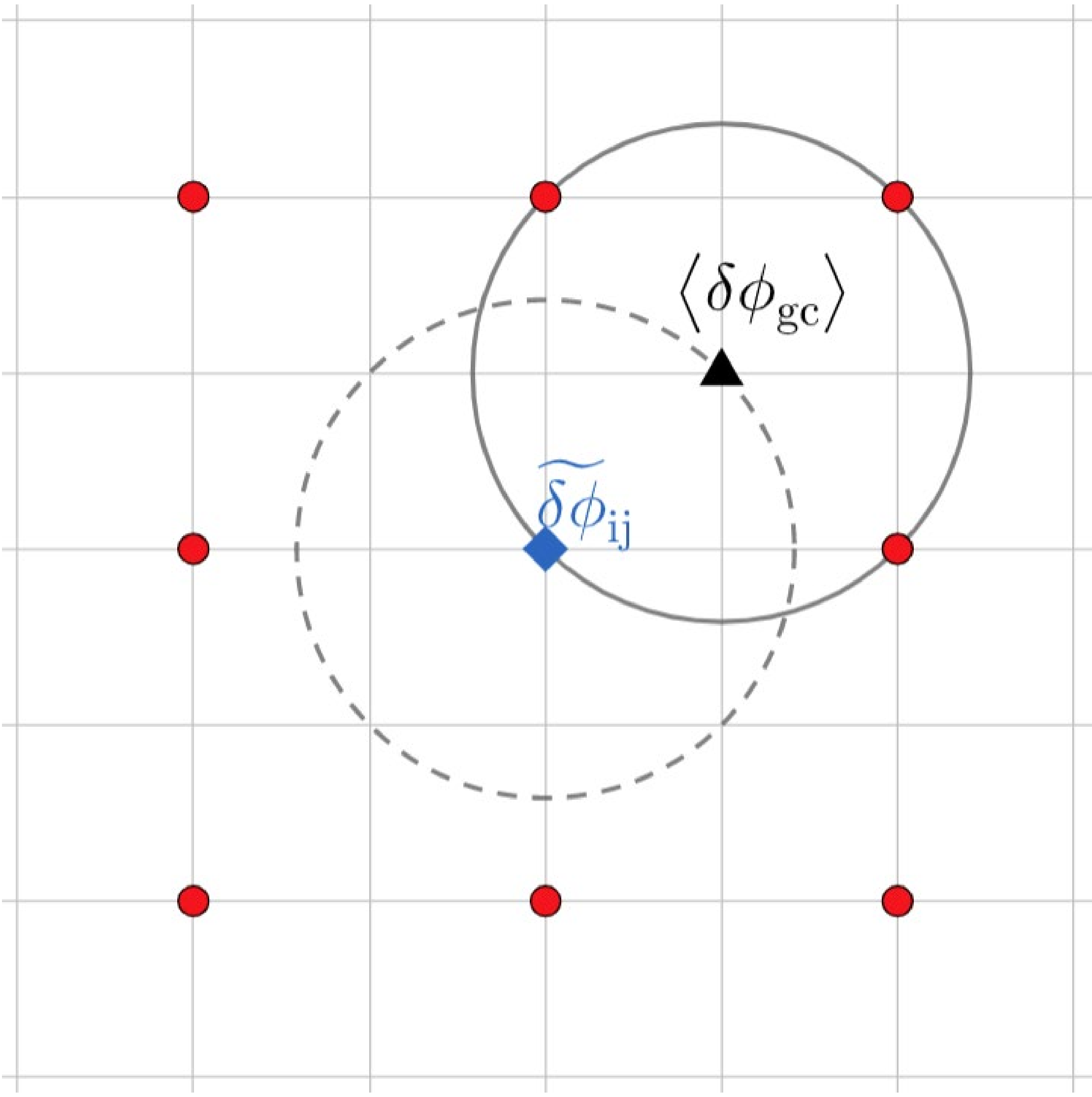

Fig. 1. Scheme for calculating $\widetilde{\delta\phi}$ at grid point $\mathbf{ij}$

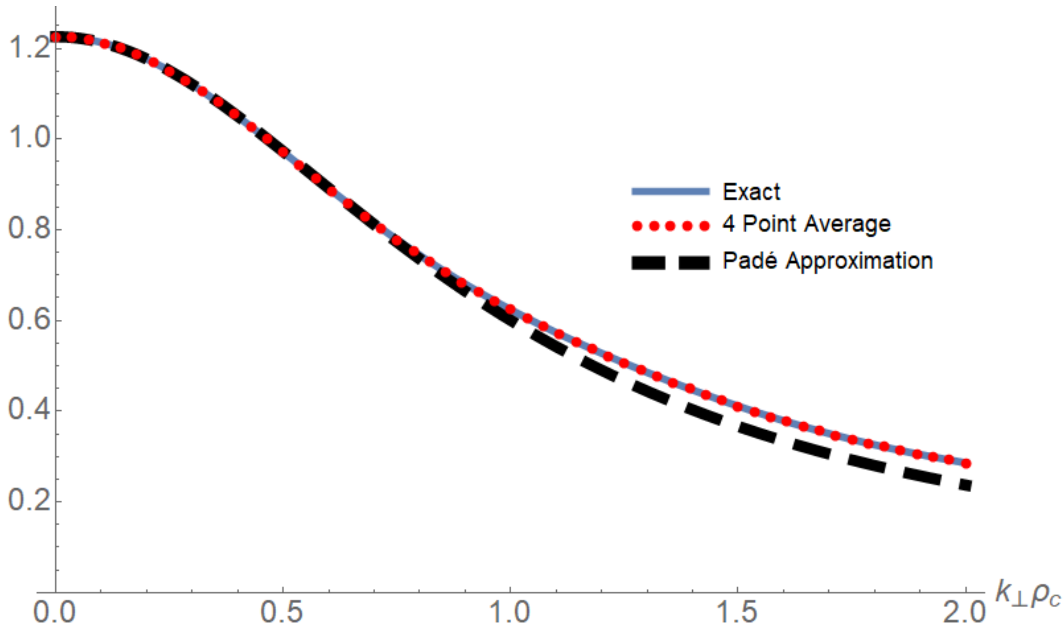

Fig. 2 Exact Γ_0 function (blue solid line) and its numerical approximations vs perpendicular wavelength $k_{\perp}\rho_c$: four-point average method with three velocity nodes in the integration (red dotted line), and Padé approximation (black dashed line).

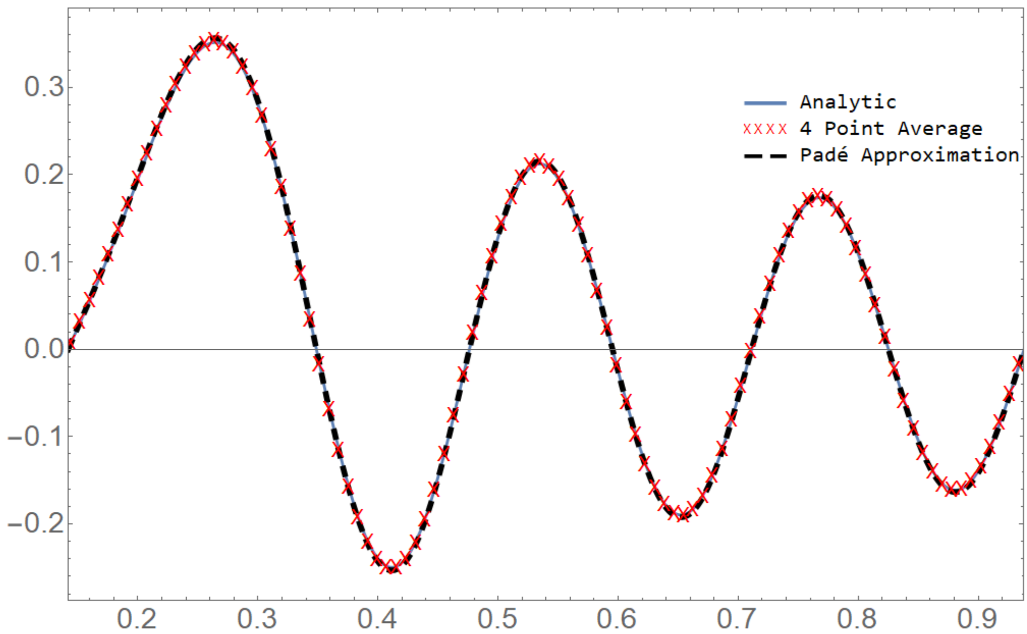

Fig. 3. Comparison of analytic expression and numeric solutions using 4-point average approximation and Pade approximation for gyrokinetic Poisson equation in the long wavelength limit with $k_r\rho_i = 0.11$ and $m = 6$.

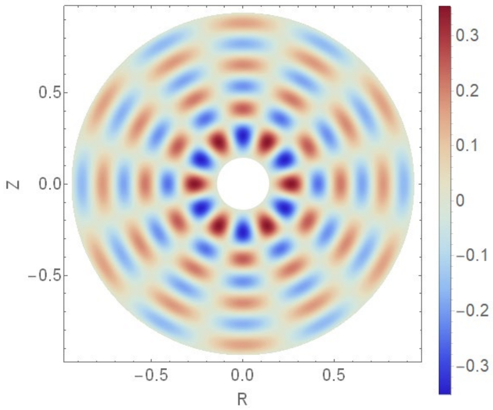

(a)

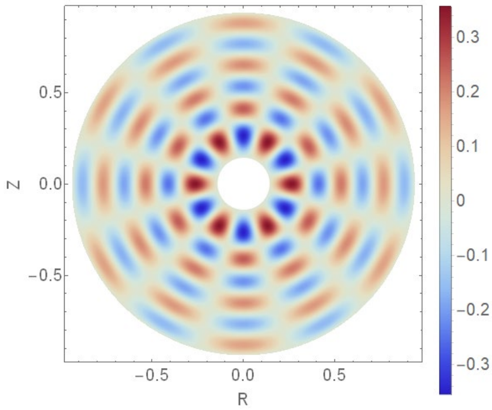

(b)

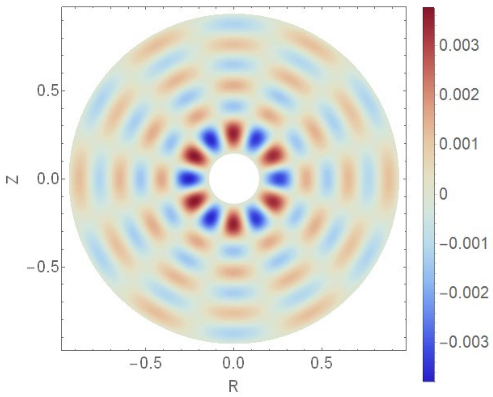

(c)

Fig. 4. 2D poloidal contours for solutions to different operators to Gyrokinetic Poisson equation in long wave length limit: (a) 4-point average operator; (b) Pade approximation operator, where $k_r \rho_i = 0.11$ and $m = 6$. The differences between these two solutions are shown in (c).

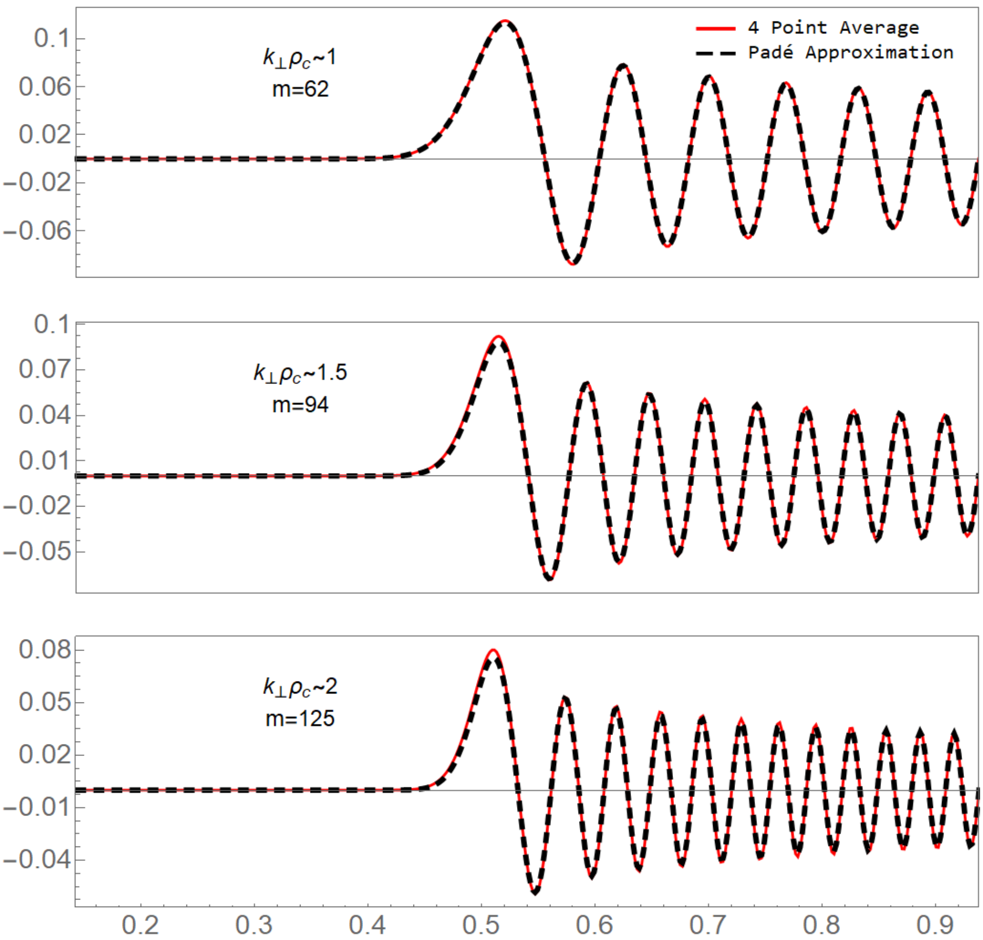

Fig. 5. Comparison between 4-point average approximation (solid line) and Pade approximation (dashed line) for the solution to Poisson equation in the short wavelength limit.

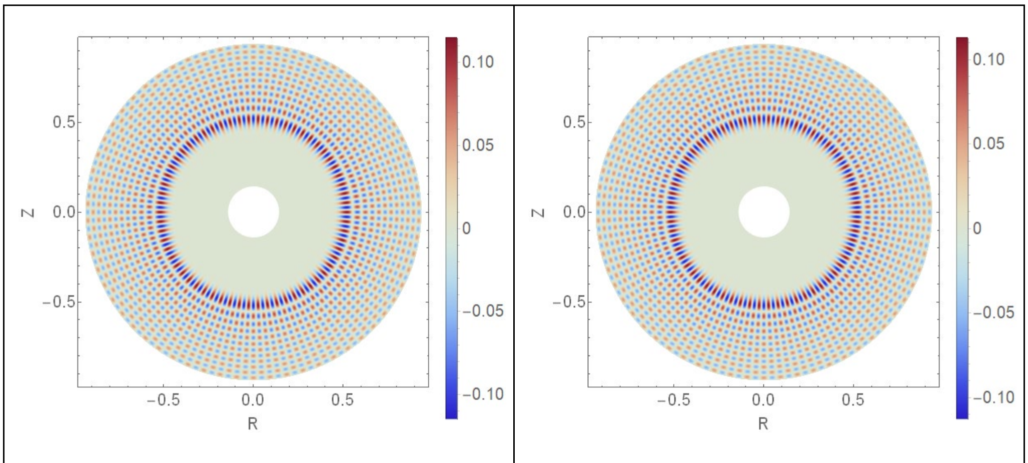

(a) 4-point average operator

(b) Pade approximation

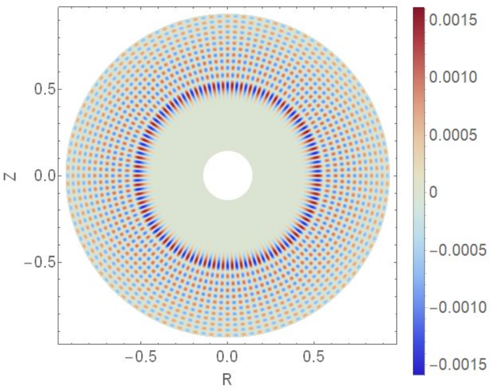

(c) Difference between Fig. 6a and Fig. 6b

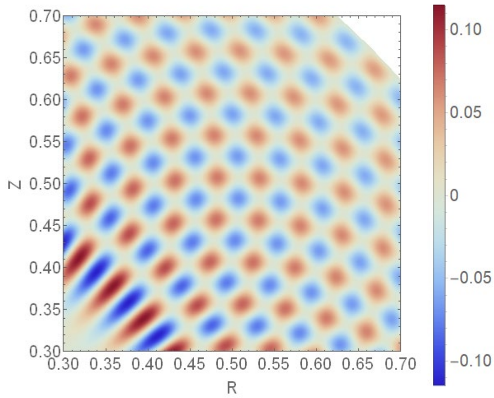

(d) Partial enlargement of Fig. 6a

Fig. 6. 2D contour of the solution to gyrokinetic Poisson equation in the short wave length limit on the poloidal plane with $\mathrm{k_r}\rho_i = 1$ and $m = 62$. The numeric operator used in solving the Poisson equation are (a) 4-point average operator, and (b) Pade approximation. The difference between them is shown in (c), and the first quadrant of (a) is enlarged in (d) to show its fine structure.